Journal of Medicinal Chemistry

Article

pubs.acs.org/jmc

N-Substituted Phenoxazine and Acridone Derivatives: Structure–Activity Relationships of Potent P2X4 Receptor Antagonists

Victor Hernandez-Olmos, Aliaa Abdelrahman, Ali El-Tayeb,† Diana Freudendahl, Stephanie Weinhausen, and Christa E. Müller*

PharmaCenter Bonn, Pharmaceutical Institute, Pharmaceutical Chemistry I, University of Bonn, An der Immenburg 4, D-53121 Bonn, Germany

Supporting Information

ABSTRACT: P2X4 receptor antagonists have potential as drugs for the treatment of neuropathic pain and neurodegenerative diseases. In the present study the discovery of phenoxazine derivatives as potent P2X4 antagonists is described. N-Substituted phenoxazine and related acridone and benzoxazine derivatives were synthesized and optimized with regard to their potency to inhibit ATP-induced calcium influx in 1321N1 astrocytoma cells stably transfected with the human P2X4 receptor. In addition, species selectivity (rat, mouse, human) and receptor subtype selectivity (versus P2X1,2,3,7) were investigated. The most potent P2X4 antagonist of the present series was *N*-(benzyloxycarbonyl)phenoxazine (**26**, PSB-12054) with an IC_{50} of 0.189 μM and good selectivity versus the other human P2X receptor subtypes. *N*-(*p*-Methylphenylsulfonyl)phenoxazine (**21**, PSB-12062) was identified as a selective P2X4 antagonist that was equally potent in all three species (IC_{50}: 0.928–1.76 μM). The compounds showed an allosteric mechanism of action. The present study represents the first structure–activity relationship analysis of P2X4 antagonists.

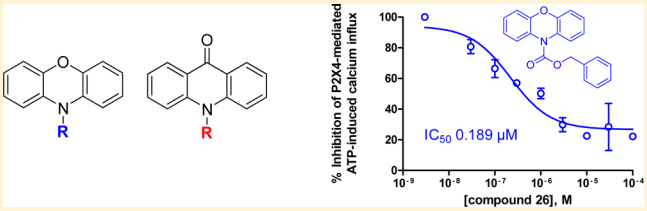

INTRODUCTION

The purine nucleotide ATP (**1**) not only is an important intracellular source of energy but also is released from the cells and activates specific cell membrane receptors. These nucleotide or P2 receptors are subdivided into two structurally distinct families: the P2X receptors (P2XR), which are ligand-gated ion channels (ionotropic receptors), and the P2Y receptors, which are G-protein-coupled (metabotropic) receptors. P2X receptors are homomeric or heteromeric cation channels permeable for Ca^{2+} and Na^{+} ions, each containing a two-transmembrane (2TM) motif.[1] Seven subunits exist, P2X1–7, with a degree of sequence identity ranging from 26% for P2X2 and P2X7 to 47% for P2X1 and P2X4. All P2X receptors are activated by ATP.[2] In contrast, the eight P2Y receptors are activated by different nucleotides depending on the receptor subtype: $P2Y_1$, $P2Y_{12}$, and $P2Y_{13}$ by ADP; $P2Y_2$ by UTP and ATP; $P2Y_4$ by UTP; $P2Y_6$ by UDP; $P2Y_{11}$ by ATP; $P2Y_{14}$ by UDP-glucose.[3] Enzymes, called ectonucleotidases, break down ATP to ADP, AMP, and adenosine and thus limit the activation of ATP receptors.[4] While adenosine activating purinergic P1 receptors (A_1, A_{2A}, A_{2B}, and A_3) show analgesic properties,[5] ATP is pronociceptive. ATP is involved in neurotransmission as a co-transmitter in all nerve types of the peripheral and central nervous system.[6,7] A remarkable functional aspect of ATP receptors, of particular therapeutic importance, is that they play a crucial role in the interaction between neurons and glia in the CNS.[8,9] Purinergic signaling has been shown to be involved in different disorders of the CNS,[10] and purinergic receptors, especially the P2X3 and P2X7 subtypes, have been advanced as targets for novel analgesics.[11] Antagonists for P2X1,[12] P2X2,[13,14] P2X3,[15,16] the heteromeric P2X2/P2X3,[16] and P2X7[17,18] receptors have been developed, and structure–activity relationships have been studied for those receptor subtypes.

Recently, the first crystal structure of a P2X receptor, the P2X4 receptor from zebra fish, has been published but without a ligand.[19] On the basis of mutagenesis and molecular modeling studies, ATP is proposed to bind to an intersubunit site around 45° from the ion channel domain, inducing conformational changes within and between subunits.[20,21]

The P2X4 receptor is highly expressed in various CNS areas, on immune cells and peripheral macrophages.[6] The location and specific up-regulation of the P2X4 receptors in CNS spinal and/or supraspinal, injury-induced, activated microglia link the receptor to pathophysiologic processes underlying persistent and neuropathic pain,[22−24] traumatic brain injury,[25] cerebral ischemia,[26] and spinal cord injury.[27] The link between up-regulation of P2X4 receptors and microglial activation points to a neuroinflammatory mechanism, the pharmacological attenuation of which may bear therapeutic potential in the treatment of chronic neuropathic pain and in neuroprotection. P2X4 receptor knockout mice showed a strong reduction in mechanical allodynia and hyperalgesia in the spinal nerve ligation model of neuropathic pain.[28]

Received: June 15, 2012
Published: October 17, 2012

However, to date, there is a lack of sufficiently powerful pharmacological tools to selectively activate or block P2X4 receptor signaling.[29] This led us to pursue the development of P2X4 antagonists in order to allow the characterization of the receptor and its (patho)physiological roles. Figure 1 shows

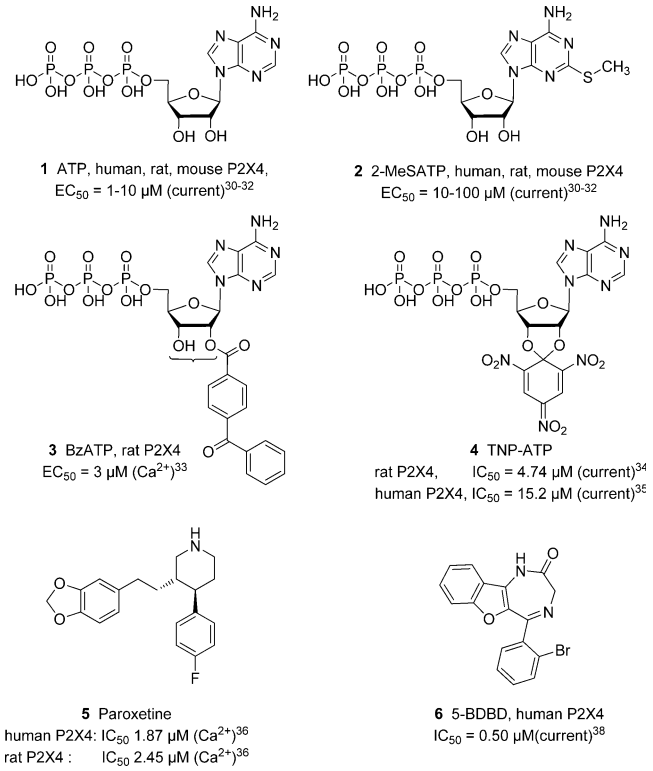

Figure 1. Structures of physiological and synthetic agonists (**1**–**3**) and antagonists (**4**–**6**) at P2X4 receptors.

some of the currently available and most frequently used P2X4 agonists and antagonists and their potency at P2X4 receptors. Besides the physiological agonist ATP (**1**),[30−32] some closely related derivatives like 2-methylthio-ATP (MeS-ATP, **2**)[30−32] and 2′(3′)-*O*-(4-benzoylbenzoyl)adenosine 5′-triphosphate (BzATP, **3**) activate the P2X4 receptor but are nonselective.[33] The ATP derivative 2′,3′-*O*-(2,4,6-trinitrophenyl)adenosine 5′-triphosphate (TNP-ATP, **4**) is a competitive antagonist.[34,35] The antidepressant drug paroxetine (**5**) was reported to be a noncompetitive P2X4 antagonist with an IC_{50} in calcium flux studies of around 2 μM at both human and rat P2X4 receptors;[36] however, Khakh and co-workers suggested an indirect effect by paroxetine, which reduced the expression of P2X4 receptors in a microglial cell line.[37] Paroxetine is much more potent as a serotonin reuptake inhibitor than as a P2X4 antagonist. Another P2X4 antagonist that has been described is 5-(3-bromophenyl)-1,3-dihydro-2*H*-benzofuro[3,2-*e*]-1,4-diazepin-2-one (5-BDBD, **6**); it was reported to block currents induced by human P2X4 receptors expressed in Chinese hamster ovary cells with an IC_{50} of 0.50 μM.[38]

So far, studies on structure−activity relationships (SARs) of P2X4 receptor antagonists have not been reported. Because of the lack of potent and selective P2X4 receptor antagonists and because of their high potential as novel therapeutics, we screened part of our in-house library (http://mueller-group.pharma.uni-bonn.de/mueller-laboratory/compound-library) to discover new scaffolds suitable for optimization. We thereby identified N-substituted phenoxazine derivatives as novel P2X4 receptor antagonists (see Figure 2 and Table 1).

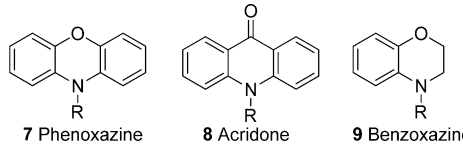

Figure 2. N-Substituted phenoxazine, acridone, and benzoxazine derivatives.

Phenoxazine and its derivatives show antioxidant properties.[39,40] N-Substituted phenoxazine derivatives have been described to possess sedative, antiepileptic, tranquillizing, spasmolytic, antitubercular, and anthelminthic activities.[41] Certain derivatives were also found to inhibit the protein kinase Akt, thereby inhibiting apoptosis of human cell lines.[42] In the present study, we describe the synthesis of a series of mostly novel N-substituted phenoxazine derivatives and structurally related benzoxazines and acridones (for basic structures see Figure 2) and their evaluation as novel P2X4 receptor antagonists. Starting from simple N-substituted phenoxazine derivatives, we explored a broad variation of N-substituents and additionally investigated a smaller series of bioisosteric acridone derivatives as well as some smaller, related bicyclic benzoxazine derivatives.

RESULTS AND DISCUSSION

Chemistry. Phenoxazine derivatives were obtained starting from phenoxazine (**7**). A wide variety of different N-substituted compounds was prepared including *N*-alkyl-, amido-, sulfonamido-, ureyl, carbamoyl-, and thiocarbamoyl-substituted derivatives (Scheme 1). *N*-Benzyl substituted phenoxazine derivative **10** was prepared by alkylation of phenoxazine using benzyl chloride in the presence of sodium hydride in tetrahydrofuran (THF), providing the desired product in 80% yield. *N*-Acetylphenoxazine derivative **11** was obtained in 43% yield by reaction of phenoxazine with sodium cyanate and acetic acid. Aromatically substituted amides **12**, **13**, and **14** were obtained by reaction of phenoxazine with the corresponding benzoic acid chloride and triethylamine in dichloroethane (DCE) (see Scheme 1), while **15** was obtained by catalytic hydrogenation of **13** with Pd/C (10%) as a catalyst. Compound **16**, with one extra carbon in the amide linker, was synthesized by treatment of phenoxazine with 2-phenylacetyl chloride in the presence of sodium hydride. The urea derivatives **17**−**20** were obtained in good yield via reaction of phenoxazine with the corresponding carbamoyl chloride and lithium diisopropylamide (LDA) in THF. The synthesis of sulfonamide derivative **21** was carried out by treatment of phenoxazine with tosyl chloride and triethylamine in DCE. Compound **22**, with one extra carbon atom in the linker, was obtained by reaction of phenoxazine with phenylmethanesulfonyl chloride in the presence of sodium hydride in THF.

Phenoxazine carbamates and thiocarbamates were obtained as shown in Scheme 1. Compound **23** was synthesized by refluxing phenoxazine in a solution of methyl chloroformate at 80 °C, while **24** was obtained using isopropyl chloroformate and performing the reaction at 110 °C. The intermediate compound phenoxazine-*N*-carbonyl chloride (**25**) was obtained from phenoxazine via reaction with triphosgene in the presence of triethylamine in DCE. Reaction of **25** with benzyl alcohol at

dx.doi.org/10.1021/jm300845v | J. Med. Chem. 2012, 55, 9576−9588

Scheme 1. Synthesis of Phenoxazine Derivatives[a]

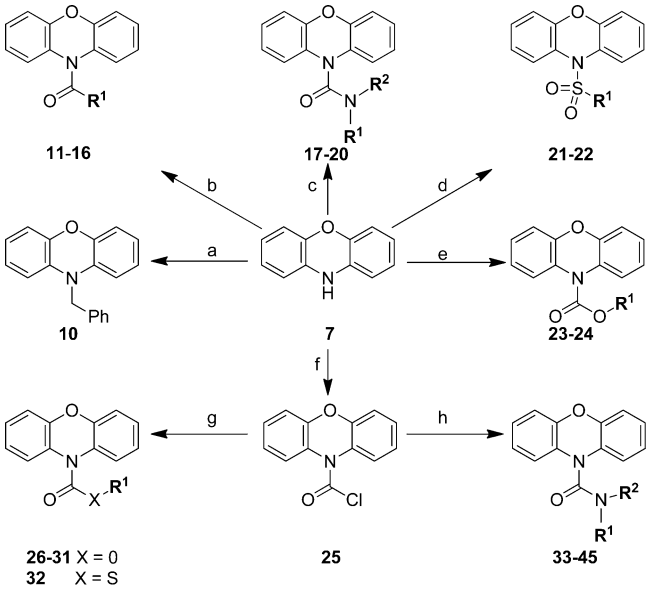

Cmpd	R^1	R^2
11	methyl	-
12	phenyl	-
13	4-nitrophenyl	-
14	4-chlorophenyl	-
15	4-aminophenyl	-
16	benzyl	-
17	methyl	methyl
18	ethyl	ethyl
19	*i*-propyl	*i*-propyl
20	R^1,R^2 = 	
21	4-methylphenyl	-
22	benzyl	-
23	methyl	-
24	*i*-propyl	-
26	benzyl	-
27	4-methylbenzyl	-
28	4-chlorobenzyl	-
29	4-nitrobenzyl	-

Cmpd	R^1	R^2
30	4-methoxylbenzyl	-
31	phenylethyl	-
32	phenylethyl	-
33	H	H
34	methyl	H
35	*i*-propyl	H
36	cyclohexyl	H
37	$-(CH_2)_3NMe_2$	H
38	4-(*N*-methylpiperidinyl)	H
39	benzyl	H
40	4-chlorobenzyl	H
41	3,5-dichlorobenzyl	H
42	phenylethyl	H
43	propyl	propyl
44	R1, R2 = 	
45	R1, R2 = 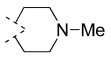	

[a]Reagents and conditions: (a) BnCl, NaH, DMF, yield 80%; (b) NaOCN, AcOH for **11**, yield 43%; R^1COCl, Et_3N, DCE for **12**–**14**, yield 44–82%; BnCOCl, NaH, THF for **16**, yield 37%; (c) LDA, THF, R^1NCOCl, yield 60–85%; (d) TsCl, Et_3N, $ClCH_2CH_2Cl$ for **21**, yield 41%; $BnSO_2Cl$, NaH, THF for **22**, yield 20%; (e) CH_3OCOCl, 70 °C for **23**, yield 81%, *i*-PrOCOCl, 110 °C for **24**, yield 50%; (f) triphosgene, $ClCH_2CH_2Cl$, Et_3N, yield 95%; (g) BnOH, 110 °C for **26**, yield 48%; NaH, THF, $R^2(CH_2)_nOH$, n = 1, 2 for **27**–**31**, yield 13–71%; NaH, THF, $BnCH_2SH$ for **32**, yield 70%; (h) 25% aqueous NH_3 for **33**, yield 96%; R^1R^2NH, DCE for **34**–**45**, yield 50–91%.

110 °C afforded **26**. Products **27**–**32** were also synthesized from intermediate **25** by treatment with the corresponding alcohol or thiol, respectively, in the presence of sodium hydride in THF (for details see Scheme 1).

A series of urea derivatives was also prepared (compounds **33**–**45**; see Scheme 1). The unsubstituted derivative **33** was obtained by treatment of phenoxazine with triphosgene and triethylamine followed by the addition of an aqueous ammonia solution. Urea derivatives **34**–**45** were obtained via **25** by treatment of **7** with triphosgene and triethylamine followed by reaction with the corresponding amine in DCE, providing the final products in moderate to good yields (Scheme 1).

A small series of structurally related acridone (**8**) derivatives was prepared as depicted in Scheme 2. Initially, there were two

Scheme 2. Synthesis of Acridone Derivatives[a]

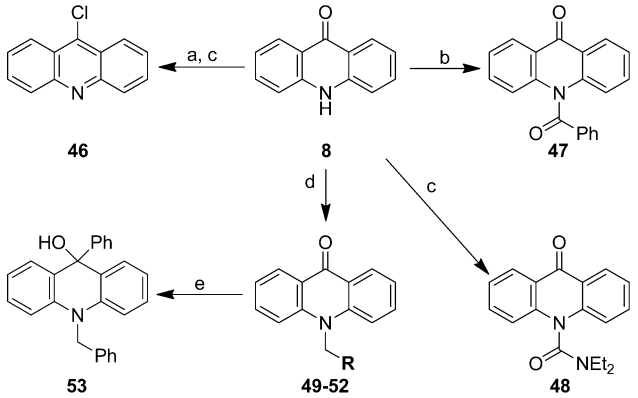

Cmpd	R
49	phenyl
50	4-methoxyphenyl
51	4-methylphenyl
52	4-nitrophenyl

[a]Reagents and conditions: (a) $ClSO_2NCO$, DCM, yield 38%; (b) BzCl, DCE, pyridine, 80 °C, yield 67%; (c) (1) triphosgene, DCE, Et_3N, (2) NH_3 25%, yield 22%; (d) RCH_2Cl, NaH, THF, yield 14–58%; (e) PhMgBr, THF, yield 64%.

synthesis attempts to obtain the acridone-*N*-carbonyl chloride derivative (the analogue of phenoxazine derivative **25**; see Scheme 1), but both were unsuccessful in our hands. In the first trial, acridone (**8**) was treated with chlorosulfonyl isocyanate in dichloromethane (DCM), but the isolated compound was identified as derivative **46**[43] (Scheme 2). In the second trial, acridone (**8**) was reacted with triphosgene in DCM in the presence of triethylamine. However, the isolated products in this case were **46** and also **48**. Benzoylacridone **47** was obtained by treatment of acridone with benzoyl chloride and pyridine in DCE at 80 °C. The alkylated derivatives **49**–**52** were obtained in low to moderate yield according to literature procedures.[44−46] Finally the tertiary alcohol **53** was prepared by a Grignard reaction from **49** in good yield (Scheme 2).[44]

As a third scaffold, bicyclic benzoxazine derivatives were prepared as phenoxazine analogues lacking the second benzene ring (Scheme 3). 2-Aminophenol (**54**) was alkylated with the respective carbonyl chlorides in the presence of calcium carbonate in dioxane. The obtained compounds **55**–**58** were further reacted with 1,2-dibromoethane in the presence of potassium carbonate to afford the corresponding cyclic analogues **59**–**61**. The morpholinyl-substituted derivative **55** was obtained in 47% yield with only traces of the dimeric byproduct. However, by use of phenyl substituted derivative **56**, benzoxazine **60** was formed in 58% yield, accompanied by 11% of the dimer **63**. The double O-alkylation rather than N-alkylation was indicated by the typical NMR shifts of the methylene hydrogens (O-alkylation, **63**, ^1H NMR (500 MHz, $CDCl_3$) δ 4.49 (s, 4H) vs N-alkylation, **60**, δ 4.40–4.33 (m, 2H), 4.05–3.97 (m, 2H)). Menthyl-substituted phenol **57** could not be converted to the benzoxazine derivative under the applied reaction conditions but afforded almost exclusively bromo derivative **62** (95% yield) after 90 h of refluxing. Benzoxazine **62** was obtained without any side products in 62% yield using carbamate **60** as a starting material.

Altogether, 52 final products were synthesized, analyzed, and tested, 36 of which are new compounds not previously described in the literature. Of the 16 previously reported

dx.doi.org/10.1021/jm300845v | *J. Med. Chem.* 2012, 55, 9576–9588

Scheme 3. Synthesis of Benzoxazine Derivatives[a]

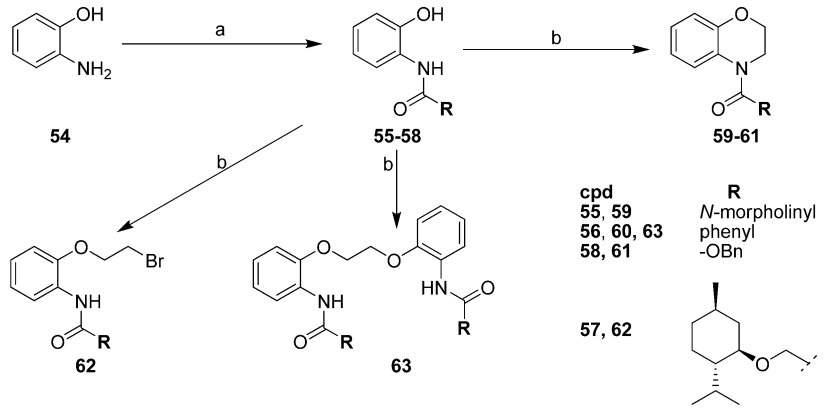

[a]Reagents and conditions: (a) carbonyl chloride, $CaCO_3$, dioxane, 70−80 °C; (b) $BrCH_2CH_2Br$, K_2CO_3, acetone, reflux, 24−90 h.

compounds, complete analytical data (^1H and ^{13}C NMR) were lacking and have now been provided. Pure compounds (≥95% purity) were mostly obtained after purification by flash chromatography. In some cases additional recrystallization was required (see Experimental Section). The structures of the synthesized compounds were confirmed by ^1H and ^{13}C NMR spectroscopy, in addition to HPLC analysis coupled to electrospray ionization mass spectrometry (LC/ESI-MS) which was also used to determine the purity.

Biological Activity. The compounds were initially tested at 10 μM for their potency to inhibit ATP-induced calcium influx in 1321N1 astrocytoma cells stably transfected with the human P2X4 receptor. For potent compounds that showed greater than 50% inhibition full concentration−response curves were determined and IC_{50} values were calculated. An ATP concentration of 1 μM, which caused ∼80% of the maximal effect, was used for receptor stimulation. Results are summarized in Table 1, and concentration−response curves for the most potent compounds are depicted in Figure 3.

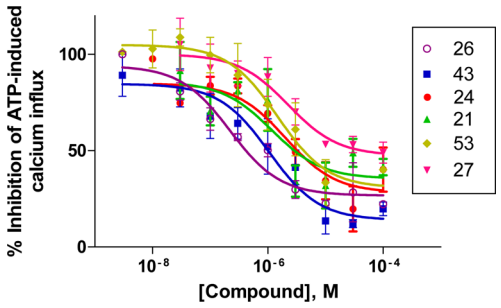

Figure 3. Concentration−response curves of selected P2X4 antagonists at human P2X4 receptors expressed in 1321N1 astrocytoma cells. Cells were preincubated for ∼30 min with test compound and subsequently stimulated with 1 μM ATP approximately corresponding to the EC_{80} of ATP. For determined IC_{50} values see Table 1.

Selected compounds were further tested at rat and mouse P2X4 receptors using the same assay system to investigate potential species differences (Table 2). Furthermore, selectivity of the most potent compounds was assessed versus the other homomeric functional human P2X receptor subtypes, P2X1, P2X2, P2X3, and P2X7, stably transfected in 1321N1 astrocytoma cells (Table 2). In order to investigate whether the potent antagonists interacted with the ATP binding site, radioligand binding studies were performed at membrane preparations of 1321N1 astrocytoma cells transfected with the human P2X4 receptor using [^{35}S]ATPγS as a radioligand (see Figure S1).

Structure−Activity Relationships. A series of 36 N-substituted phenoxazine derivatives were investigated (compounds **10**−**45**; see Table 1). A substituent was connected to the nitrogen atom of phenoxazine via one of the following linkers: (i) one-atom linkers, including methylene (−CH_2), carbonyl (−C═O) yielding amides, or sulfonyl (−SO_2) yielding sulfonamides and (ii) two-atom linkers, including −CONH yielding ureas, −C(O)O yielding carbamates, or −C(O)S yielding thiocarbamates.

A simple *N*-benzyl-substituted phenoxazine (**10**) was virtually inactive (14% inhibition at 10 μM). Replacement of the methylene linker in **10** by a carbonyl group (yielding compound **12**) strongly increased P2X4-antagonistic potency, resulting in an IC_{50} of 4.11 μM. Therefore, amides were further explored. Smaller residues instead of phenyl such as Cl (in **25**) or methyl (in **11**) clearly reduced inhibitory potency. The same was observed with the larger benzyl group (in **16**), which was not tolerated by the receptor, in contrast to a smaller phenyl ring (compound **12**). *p*-Substitution of the phenyl residue in **12** was explored, and *p*-nitrobenzoyl- (**13**), *p*-chlorobenzoyl- (**14**), and *p*-aminobenzoyl- (**15**) substituted phenoxazine derivatives were investigated. Compounds **13** and **14** bearing electron-withdrawing groups showed about the same potency as the unsubstitued benzoylphenoxazine (**12**). The aminobenzoyl-substituted derivative **15** was slightly less potent exhibiting an IC_{50} of 10.8 μM. Two sulfonamide derivatives were prepared (**21** and **22**). The test results showed that the carbonyl linker could be bioisosterically replaced by a sulfonyl function. While benzyl derivative **22** showed moderate potency (46% inhibition of ATP-induced calcium influx at 10 μM), similar or perhaps slightly better than the corresponding benzyl derivative of the carbonyl series (compound **16**, 31% inhibition at 10 μM), the *p*-methylphenyl-substituted sulfonamide derivative **21** was a potent P2X4 antagonist exhibiting an IC_{50} of 1.38 μM (Table 1).

Next we explored two-atom linkers (urea and (thio)-carbaminic acid ester derivatives); most investigated examples belonged to this second group of compounds. The unsubstituted phenoxazinecarboxamide, the urea derivative **33**, showed only low potency (40% inhibition at 10 μM).

dx.doi.org/10.1021/jm300845v | J. Med. Chem. 2012, 55, 9576−9588

Table 1. Potency of Phenoxazine, Acridone, and Benzoxazine Derivatives at Human P2X4 Receptors

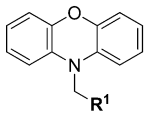

10

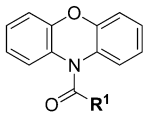

11-16, 25

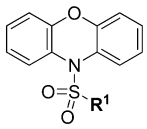

21-22

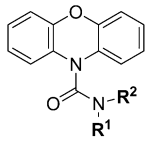

17-20, 33-45

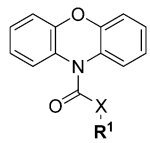

23, 24, 26-31 X = O
32 X = S

Compd.	R^1	R^2	Human P2X4 IC_{50} ± SEM[a] (μM)
Benzyl derivative			
10	phenyl	-	>10 (14%)[b]
Amides			
25	chloro	-	23.2 ± 8.8 (85%)[c]
11	methyl	-	>10 (23%)[b]
12	phenyl	-	4.11 ± 1.59 (54%)[c,d]
13	4-nitrophenyl	-	4.29 ± 1.49 (51%)[c,d]
14	4-chlorophenyl	-	5.29 ± 2.57 (49%)[c,d]
15	4-aminophenyl	-	10.8 ± 0.8 (95%)[c]
16	benzyl	-	>10 (31%)[b]
Sulfonamides			
21 (PSB-12062)	4-methylphenyl	-	1.38 ± 0.33 (68%)[c,d]
22	benzyl	-	≥10 (46%)[b]
Ureas			
33	H	H	≥10 (40%)[b]
34	methyl	H	≥10 (37%)[b]
35	*i*-propyl	H	>10 (13%)[b]
36	cyclohexyl	H	>10 (28%)[b]
37	$-(CH_2)_3NMe_2$	H	>10 (7%)[b]
38	4-(*N*-methylpiperidinyl)	H	45.8 ± 11.3 (94%)[c]
39	benzyl	H	>10 (15%)[b]
40	4-chlorobenzyl	H	9.54 ± 3.29 (95%)[c]
41	3,5-dichlorobenzyl	H	>10 (24%)[b]
42	2-phenylethyl	H	1.78 ± 0.28 (66%)[c,d]
17	methyl	methyl	24.6 ± 6.7 (64%)[c]
18	ethyl	ethyl	17.4 ± 4.6 (79%)[c]
43	propyl	propyl	2.69 ± 0.38 (80%)[c]
19	*i*-propyl	*i*-propyl	12.4 ± 1.7 (104%)[c]
20			>>10 (0%)[b]
44			10.7 ± 1.9 (55%)[c,d]
45			>>10 (0%)[b]

dx.doi.org/10.1021/jm300845v | *J. Med. Chem.* 2012, 55, 9576−9588

Table 1. continued

Compd.	R^1	R^2	Human P2X4 $IC_{50} \pm SEM^a$ (μM)
Carbamates			
23	methyl	-	52.3 ± 11.7 (91%)[c]
24	*i*-propyl	-	2.35 ± 0.71 (60%)[c]
26 (PSB-12054)	benzyl	-	0.189 ± 0.059 (77%)[b]
27	4-methylbenzyl	-	2.28 ± 0.58 (51%)[c,d]
28	4-chlorobenzyl	-	1.02 ± 0.31 (69%)[c,d]
29	4-nitrobenzyl	-	>>10 (0%)[b]
30	4-methoxybenzyl	-	2.64 ± 0.38 (49%)[c,d]
31	2-phenylethyl	-	3.93 ± 0.89 (85%)[c]
32	2-phenylethyl	-	≥10 (39%)[b]

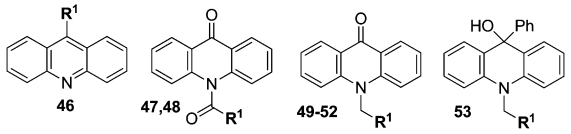

Compd	R^1	R^2	Human P2X4 $IC_{50} \pm SEM^a$ (μM)
46	chloro	-	>10 (28%)[b]
47	phenyl	-	26.9 ± 6.4 (84%)[c]
48	NEt_2	-	39.1 ± 7.5 (85%)[c]
49	phenyl	-	5.97 ± 2.17 (75%)[c]
50	4-methoxyphenyl	-	10.3 ± 2.69 (76%)[c]
51	4-methylphenyl	-	11.8 ± 3.93 (92%)[c]
52	4-nitrophenyl	-	2.49 ± 1.52 (95%)[c]
53	phenyl	-	2.44 ± 1.05 (67%)[b,d]

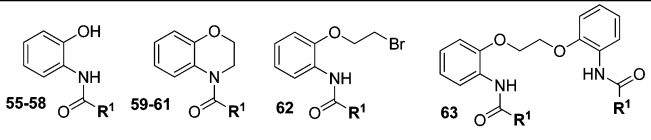

Compd	R^1	R^2	Human P2X4 $IC_{50} \pm SEM^a$ (μM)
55	morpholinyl	-	>10 (26%)[b]
56	phenyl	-	>10 (18%)[b]
57	-OCH_2-(-)-menthyl	-	3.39 ± 0.77 (77%)[c]
58	OBn	-	>>10 (7%)[b]
59	*N*-morpholinyl	-	>>10 (2%)[b]

dx.doi.org/10.1021/jm300845v | *J. Med. Chem.* 2012, 55, 9576−9588

Table 1. continued

Compd	R^1	R^2	Human P2X4 $IC_{50} \pm SEM^a$ (μM)
60	phenyl	-	>>10 (3%)[b]
61	OBn	-	>10 (28%)[b]
62	-OCH_2-(-)-menthyl	-	>10 (13%)[b]
63	phenyl	-	>>10 (0%)[b]

[a] $n = 3$ unless otherwise noted. [b] Percent inhibition at 10 μM test compound. [c] Percent inhibition at 100 μM test compound. [d] Percent inhibition at IC_{50} was significantly lower than 50%: **12**, 37%; **13**, 27%; **14**, 15%; **21**, 39%; **27**, 27%; **28**, 39%; **30**, 21%; **42**, 35%; **44**, 36%; **53**, 35%.

Monosubstitution with alkyl residues including methyl (**34**), isopropyl (**35**), cyclohexyl (**36**), (*N*,*N*-dimethylamino)ethyl (**37**), or 4-(*N*-methylpiperidinyl) (**38**) did not improve the potency of the urea derivatives.

In contrast, N,N-disubstitution with small alkyl residues resulted in the following sequence of potency: dimethyl (**17**, IC_{50} = 24.6 μM) ≤ diethyl (**18**, 17.4 μM) ≤ diisopropyl (**19**, 12.4 μM) < dipropyl (**43**, 2.69 μM). The piperidine derivative **44**, which can be envisaged as a sterically fixed analogue of the potent dipropyl derivative **43**, was about 3-fold less potent (IC_{50} = 10.7 μM). The analogous morpholine (**20**) and *N*-methylpiperazine derivative (**45**) were completely inactive indicating that a polar function is not tolerated.

Benzyl substitution was not well tolerated in the urea series (compound **39**), but *p*-chloro substitution of the benzyl ring increased potency (**40**, IC_{50} = 9.54 μM), while the 3,5-dichloro-substituted derivative **41** was inactive. However the larger 2-phenylethyl substitution (compound **42**) resulted in a potent P2X4 antagonist with an IC_{50} of 1.78 μM.

The second series of compounds with a two-atom linker were the carbamates **23**, **24**, and **26**−**31** and the thiocarbamate **32** (Table 1). They are analogues of the urea derivatives in which the exocyclic nitrogen atom is replaced by an oxygen or a sulfur atom. However, the structure−activity relationships were quite different in the carbamate series compared to the urea series of compounds. In contrast to the ureas, monosubstitution with small alkyl residues was tolerated in the carbamate series: the methyl ester (**23**) was weak (IC_{50} = 52.3 μM), but the isopropyl ester (**24**) showed high potency exhibiting an IC_{50} of 2.35 μM. Also contrary to the results with the urea derivatives, the unsubstituted benzylcarbamate (**26**; compare to urea derivative **39**) was a very potent antagonist; in fact **26** was the most potent P2X4 antagonist of the present series with an IC_{50} of 0.189 μM. *p*-Substitution did not further increase its potency, but *p*-methyl- (**27**, IC_{50} = 2.28 μM), *p*-methoxy- (**30**, IC_{50} = 2.64 μM), and *p*-chloro-substitution (**28**, IC_{50} = 1.02 μM) were well tolerated resulting in compounds with IC_{50} values in the low micromolar range, while a *p*-nitro group (in **29**) abolished activity. The larger 2-phenylethyl residue (in **31**, IC_{50} = 3.93 μM) was also well tolerated but did not increase potency in the carbamate series in comparison to the benzyl residue, as it had in the urea series of phenoxazine derivatives. The corresponding 2-phenylethyl-substituted thiocarbamate **32** was even less potent.

As a related heterotricyclic scaffold a small series of acridone derivatives and closely related analogues was investigated (**46**−**53**). 6-Chloroacridine (**46**) was inactive. *N*-Benzoylacridone (**47**) showed moderate potency (IC_{50} = 26.9 μM). In comparison to the corresponding phenoxazine derivative **12** (IC_{50} = 4.11 μM) it was almost 7-fold less potent. Similarly, the *N*,*N*-diethyl-substituted urea derivative **48** (IC_{50} = 39.1 μM) was somewhat less potent than the corresponding phenoxazine derivative **18**. In contrast, *N*-benzylacridone (**49**) was relatively potent (IC_{50} = 5.97 μM), while the corresponding *N*-benzylphenoxazine (**10**) had been inactive. *p*-Substitution of the benzyl residue did significantly alter the potency of the acridones (compounds **50**−**52**); *p*-nitro-substitution resulted in the most potent compound of this series (**52**, IC_{50} = 2.49 μM). Virtually the same potency was observed for the N1-benzyl-substituted 6-hydroxy-6-phenyldihydroacridine (**53**, IC_{50} = 2.44 μM).

A third series of heterocyclic scaffolds that was investigated was the bicyclic benzoxazine derivatives, which are related to phenoxazines but are lacking one of the benzene rings. The oxazine ring in the investigated compounds **59**−**61** was partially hydrogenated (see Table 1). In fact, all three investigated derivatives, including the benzylcarbamate **61**, the analogue of the corresponding phenoxazine derivative **26**, which had been the most potent compound in that series, were inactive at P2X4 receptors. Several intermediate and side products obtained during the efforts to synthesize benzoxazine derivatives were also tested (**55**−**58**, **62**, and **63**; Table 1). All of them were inactive except for one compound, the *o*-hydroxyphenylcarbamate **57** (IC_{50} = 3.39 μM), which is substituted with a bulky chiral (−)-menthyl residue. This result indicates that voluminous residues are tolerated by the P2X4 receptor like it had previously been shown for the P2X7 receptor.[47] Thus, compound **57** may serve as a new lead structure for further optimization.

Some of the compounds did not lead to complete inhibition of the ATP-induced calcium signal even at high concentrations, and this did not correlate with their potency (see Figure 3 and Table 1 where the percent inhibition at 100 μM is provided). For example, the most potent antagonist **26** showed a maximal inhibition of 77%, while the weaker compound **19** showed complete inhibition at a high concentration of 100 μM. Incomplete inhibition may indicate an allosteric mode of action. When percent inhibition of the compounds at their IC_{50} was considered, two-thirds of the compounds showed nearly 50% inhibition (49 ± 7%, 95% confidence interval of 45−53%). One-third of the compounds, **12**, **13**, **14**, **21**, **27**, **28**, **30**, **42**, **44**, and **53**, showed significantly lower inhibition between 15% and 39% at their IC_{50} value. This was reflected by a maximal inhibition of only around 50−70% at a high concentration of 100 μM. However, clear SARs for partial versus full inhibition of P2X4-receptor induced calcium influx could not be deduced.

dx.doi.org/10.1021/jm300845v | *J. Med. Chem.* 2012, 55, 9576−9588

Table 2. Potency of Selected Derivatives at P2X4 Orthologues and Different P2X Receptor Subtypes

	IC_{50} ± SEM (μM)						
compd	human P2X4	rat P2X4	mouse P2X4	human P2X1	human P2X2	human P2X3	human P2X7
TNP-ATP (**4**)	1.46 ± 0.29	4.71 ± 0.71	1.28 ± 0.01	nd[b]	nd[b]	nd[b]	nd[b]
21	1.38 ± 0.33	0.928 ± 0.512	1.76 ± 1.09	≥10 (45%)[a]	>10 (−5%)[a]	>10 (32%)[a]	>10 (6%)[a]
24	2.35 ± 0.71	6.08 ± 1.52	>10 (1%)[a]	≥10 (38%)[a]	>10 (13%)[a]	>10 (11%)[a]	>10 (10%)[a]
26	0.189 ± 0.059	2.10 ± 1.09	1.77 ± 0.34	6.52 ± 1.68	>10 (13%)[a]	~10 (49%)[a]	>10 (9%)[a]
27	2.28 ± 0.58	>10 (24%)[a]	2.81 ± 0.51	>10 (24%)[a]	>10 (−84%)[a,c]	>10 (8%)[a]	>10 (29%)[a]
42	1.78 ± 0.28	≥10 (42%)[a]	>10 (5%)[a]	>10 (23%)[a]	>10 (27%)[a]	>10 (4%)[a]	>10 (13%)[a]
43	2.69 ± 0.38	≥10 (36%)[a]	2.71 ± 1.21	2.02 ± 0.80	>10 (33%)[a]	≥10 (44%)[a]	>10 (2%)[a]
53	2.44 ± 1.05	4.04 ± 1.22	2.66 ± 0.57	0.602 ± 0.169	≥10 (46%)[a]	0.429 ± 0.141	1.27 ± 0.36

[a]Inhibition of calcium flux at 10 μM. [b]Not determined. [c]Compound significantly increased ATP effect (positive modulator).

Species Selectivity. For some classes of P2X (e.g., P2X7) receptor antagonists, large species differences between potencies at human versus rodent P2X receptors have been described.[48] Therefore, we investigated selected compounds of the new series of P2X4 antagonists at rat and mouse, in addition to human P2X4 receptors in calcium influx assays determining the antagonist-induced inhibition of ATP-mediated receptor activation (Table 2). For comparison, the known P2X4 antagonist TNP-ATP (**4**), an ATP derivative, was also included. TNP-ATP did not show any significant species differences, being similarly potent at human (IC_{50} = 1.46 μM) and mouse P2X4 receptors (IC_{50} = 1.28 μM) and only slightly (3-fold) less potent at rat P2X4 receptors (IC_{50} = 4.71 μM).

Six of the most potent phenoxazine derivatives were investigated at P2X4 receptors of all three species: the sulfonamide **21**, the carbamates **24**, **26**, and **27**, and the urea derivatives **42** and **43**. In addition, the acridine derivative **53** was investigated. The latter did not show any species differences but inhibited P2X4 receptors across species with nearly identical IC_{50} values. The same was true for *N*-(*p*-methylphenylsulfonyl)phenoxazine (**21**). In contrast, the other phenoxazine derivatives, carbamate as well as urea derivatives, exhibited some species selectivity. Compounds **24** (isopropylcarbamate derivative) and **42** (phenylethylurea derivative) were somewhat weaker at rat and nearly inactive at mouse P2X4 receptors than at the human orthologue. The *p*-methylbenzylcarbamate **27** and the *N*,*N*-dipropylurea derivative **53** were equipotent at human and mouse receptors but much weaker at the rat P2X4 receptor. These results showed that species differences may be common for P2X4 receptor antagonists, and new ligands have to be characterized at the species of interest before they are being used as pharmacological tools.

Receptor Selectivity. In order to assess the selectivity of the new P2X4 receptor antagonists versus closely related targets, selected compounds were tested in calcium influx assays at the other functional homomeric human P2X receptor subtypes, namely, P2X1, P2X2, P2X3, and P2X7, at 10 μM (see Table 2). Most of the compounds showed good selectivity for the P2X4 receptor. For example, the most potent antagonist of the present series, phenoxazine derivative **26**, was at least 35-fold selective versus all other human P2X receptor subtypes. There were two exceptions: the phenoxazine derivative **43**, which was equipotent at P2X1 receptors, and the dihydroacridine derivative **53**, which was nonselective inhibiting all P2X receptor subtypes at 0.429 μM (P2X3), 0.602 μM (P2X1), 1.27 μM (P2X7), 2.44 μM (P2X4), and ~10 μM (P2X2) (see Table 2, Figure 4). These results indicate that starting points can be found to develop phenoxazine and acridine derivatives as antagonists for other P2X receptor subtypes as well.

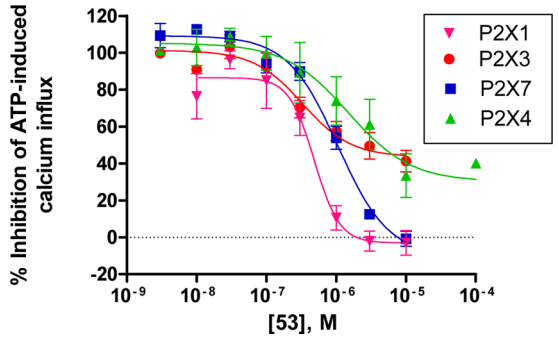

Figure 4. Concentration-dependent inhibition of ATP-induced calcium influx by compound **53** at different human P2X receptor subtypes. For IC_{50} values see Table 2. An ATP concentration corresponding to the EC_{80} was used.

Phenoxazine **27** (a *p*-methylbenzylcarbamate) showed a peculiar effect at the P2X2 receptor: it did not inhibit ATP-induced receptor activation but had the opposite effect − it significantly enhanced the ATP effect (by 84% at 10 μM; ATP concentration of 1 μM corresponding to the EC_{80}). This effect was highly reproducible. Compound **27** can thus be characterized as a positive allosteric modulator (PAM) at P2X2 receptors.

The two most potent P2X4 receptor subtype-selective phenoxazine derivatives **21** and **26** were additionally investigated at a panel of 80 important drug targets comprising a variety of receptors, ion channels, and transporters (http://www.cerep.fr/cerep/users/pages/catalog/Assay/catalog.asp). At 10 μM both compounds showed no significant interaction with the majority of the investigated targets (see Supporting Information). Compound **21** only showed significant affinity for 2 of the 80 investigated targets, namely, adenosine A_3 and benzodiazepine receptors (>80% inhibition at 10 μM), while compound **26** only showed significant binding to one target: serotonin 5-HT_{2B} receptors (for details see Supporting Information). Thus, both compounds appear to be relatively selective for P2X4 receptors.

Radioligand Binding Studies. The new P2X4 receptor antagonists may exhibit a competitive mechanism of inhibition interacting with the ATP binding site, or they may modulate ATP binding by interacting with an allosteric site on the receptor. In order to investigate their potential interaction with the ATP binding site, radioligand binding studies (competition assays) were performed using [^{35}S]ATPγS as a radioligand.[49] Results for all tested compounds (**21**, **24**, **26**, **27**, **42**, **43**, **53**) are shown in Supporting Information (Figure S5). None of the compounds competed with the binding of ATP in the

dx.doi.org/10.1021/jm300845v | J. Med. Chem. 2012, 55, 9576−9588

concentration range where they inhibited functional receptor response. Only at very high concentrations (>10 μM) compounds **21** and **24** appeared to reduce radioligand binding. In contrast, the ATP derived P2X4 antagonist ATP-TNP (**4**) inhibited the binding of [^{35}S]ATPγS in a concentration-dependent manner showing a low K_i of 48.9 ± 11.1 nM. These results clearly show that the ATP derivative **4** is a competitive antagonist, while the new antagonists described in the present study appear to act as negative allosteric modulators showing a noncompetitive mechanism of action. This is in agreement with the lipophilic nature of the developed P2X4 antagonists, while orthosteric ligands are expected to be polar, negatively charged molecules. It will therefore in general be easier to develop P2X4 antagonists with druglike properties that interact with allosteric sites than with the positively charged ATP-binding site. On the other hand, some of the most potent compounds of the present series possess low water solubility. The sulfonamide derivative **21** was less lipophilic and more water-soluble than the carbamate **26**. In the future we will therefore introduce solubilizing function and extend the series of sulfonamide derivatives.

Investigation of Hydrolytic Stability. Since carbamates may be hydrolytically unstable, stability tests were performed for the most active compound of the series, carbamate **26**, at three different pH values. In the first experiment, a 100 μM solution of **26** in DMSO/HCl (aq, pH 1, 1:4) was stirred for 6 h at room temperature. In the second experiment, a 100 μM solution of **26** in DMSO/HBSS buffer, pH 7.4 (1:4), was stirred for 6 h at 80 °C. In the third experiment a 10 μM solution of **26** in DMSO/$NaHCO_3$ (aq, pH 8.4, 2.5:97.5) was stirred for 6 h at 37 °C. In all three cases LC−MS analyses showed no degradation of **26**. These results confirm the hydrolytic stability of the carbamate group of phenoxazine derivative **26** under neutral conditions as they are found in blood, under acidic conditions, as present in the stomach, and under basic conditions, which are found in the intestine.

CONCLUSIONS

N-Substituted phenoxazine and related acridone derivatives have been discovered as potent and selective allosteric P2X4 receptor antagonists. The present study represents the first SAR study of P2X4 antagonists. Structural optimization resulted in the development of several compounds that will be useful as pharmacological tools. The most potent P2X4 antagonist of the present series was *N*-(benzyloxycarbonyl)phenoxazine (**26**, PSB-12054) with an IC_{50} of 0.189 μM at human P2X4 receptors, maximal receptor inhibition of 77%, and good selectivity versus the other human P2X receptor subtypes. The compound was shown to possess hydrolytic stability at neutral and acidic pH values. *N*-(*p*-Methylphenyl)sulfonylphenoxazine (**21**, PSB-12062) was identified as a potent and selective P2X4 antagonist that was about equally active at P2X receptors of different species (IC_{50}: rat, 0.928 μM; mouse, 1.76 μM; human, 1.38 μM, maximal inhibition of 68%). *N*10-Benzyl-9-phenyl-9,10-dihydroacridine-9-ol (**53**) was found to be a potent P2X4 antagonist (IC_{50} = 2.44 μM) but showed even higher potency at human P2X3 (IC_{50} = 0.429 μM) and P2X1 (IC_{50} = 0.602 μM) receptors and thus may be a new starting point for the development of potent and selective P2X1 and/or P2X3 receptor antagonists. *N*-(*p*-Methylbenzyloxycarbonyl)-phenoxazine (**27**), a potent and selective P2X4 receptor antagonist, was found to be also a positive allosteric modulator of P2X2 receptor function. Some of the newly identified P2X4 receptor antagonists possess higher affinity than the best antagonists described so far in the literature (compounds **5** and **6**). Furthermore, compounds **21** and **26** have also shown good selectivity versus the other P2X receptor subtypes. The phenoxazine and acridone derivatives can be obtained by simple, straightforward syntheses, and these structural classes of compounds still present room for further optimization with regard to affinity and improvement of their physicochemical properties. The new P2X4 receptor antagonists will be further optimized, and their usefulness as pharmacological tools for in vitro and in vivo studies will be investigated in due course.

EXPERIMENTAL SECTION

General. All commercially available reagents were obtained from various producers (Acros, Alfa Aesar, and Sigma-Aldrich) and used without further purification. Solvents were used without additional purification or drying unless otherwise noted. The reactions were monitored by thin layer chromatography (TLC) using aluminum sheets with silica gel 60 F_{254} (Merck). Column chromatography was carried out with silica gel 0.060−0.200 mm, pore diameter of ∼6 nm. ^{1}H and ^{13}C NMR data were collected on a Bruker Avance 500 MHz NMR spectrometer at 500 MHz (^{1}H) and 126 MHz (^{13}C), respectively. $CDCl_3$ was used as a solvent. Chemical shifts are reported in parts per million (ppm) relative to the deuterated solvent, that is, δ ^{1}H, 7.26 ppm; ^{13}C, 70.0 ppm. Coupling constants *J* are given in hertz, and spin multiplicities are given as s (singlet), d (doublet), t (triplet), q (quartet), m (multiplet), br (broad). Melting points were determined on a Büchi 530 melting point apparatus and are uncorrected. The purities of isolated products were determined by ESI mass spectra obtained on an LC−MS instrument (Applied Biosystems API 2000 LC−MS/MS instrument, HPLC Agilent 1100 instrument) using the following procedure. The compounds were dissolved at 0.5 mg/mL in H_2O/MeOH = 1:1, containing 2 mM ammonium acetate. Then 10 μL of the sample was injected into an HPLC column (Phenomenex Luna 3 μm C18, 50 mm × 2.00 mm). Elution was performed with a gradient of water/methanol (containing 2 mM ammonium acetate) from 90:10 to 0:100 for 30 min at a flow rate of 250 μL/min, the gradient starting after 10 min. UV absorption was detected from 200 to 950 nm using a diode array detector. Purity of all compounds was determined at 254 nm. The purity of the compounds was generally ≥95%.

Compounds **49**,[44] **50**,[45] **52**,[46] and **53**[44] were synthesized as described in the literature. Compounds **10**,[50] **11**,[51] **13**,[52] **21**,[53] **23**,[54] **25**,[55] **44**,[54] **46**,[43] **47**,[56] **55**,[57] **56**,[58] **58**,[59] and **60**[60] have previously been described but were obtained by new methodologies, and additional structural characterization data are provided in the present study (for detailed synthesis and experimental data see Supporting Information).

General Procedure for the Synthesis of Compounds 12−14. Benzoyl chloride (163 μL, 1.4 mmol) was added to a solution of phenoxazine (187 mg, 1.0 mmol) and triethylamine (209 μL, 1.5 mmol) in dichloroethane (DCE, 3 mL) at 0 °C under argon. The resulting mixture was stirred at room temperature for 2 h. Then the reaction was quenched with aqueous HCl solution (20 mL, 0.5 M), and the aqueous portion was extracted with dichloromethane (DCM) (3 × 20 mL). The organic layers were combined, dried over $MgSO_4$, and subsequently evaporated. Pure compounds were isolated after flash chromatography (for conditions see the individual compounds) and crystallized (for crystallization solvents see the individual compounds).

General Procedure for the Synthesis of Compounds 17−20. To a solution of lithium diisopropylamide (LDA, 1 mL, 2 M in tetrahydrofuran (THF), 2 mmol) was added a solution of phenoxazine (187 mg, 1 mmol) and the corresponding carbamoyl chloride (2.5 mmol) in dry THF (3 mL) at 0 °C under an argon atmosphere. The mixture was allowed to warm to room temperature and stirred for 2 h. Then the reaction was quenched with aqueous HCl (30 mL, 0.4 M), and the aqueous portion was extracted with DCM (3 × 20 mL). The combined organic layers were washed with brine (50 mL) and dried

dx.doi.org/10.1021/jm300845v | J. Med. Chem. 2012, 55, 9576−9588

over $MgSO_4$. Pure compounds were isolated after flash chromatography (for conditions see the individual compounds) and crystallized (for crystallization solvents see the individual compounds).

General Procedure for the Synthesis of Compounds 23 and 24. A solution of phenoxazine (187 mg, 1 mmol) in the corresponding chloroformate (3 mL) was heated at 75 °C for compound **23** and at 110 °C for compound **24** for 3.5 h. Then the mixture was diluted with DCM (60 mL) and washed with saturated aqueous $NaHCO_3$ solution (20 mL) and brine (20 mL). The organic phase was dried over $MgSO_4$ and evaporated. Pure compounds were isolated after crystallization (for crystallization solvents see the individual compounds).

General Procedure for the Synthesis of Compounds 26−31. To a suspension of NaH (60% in mineral oil, 1 mmol, 40 mg) in dry THF (1 mL) was added the corresponding alcohol (0.87 mmol), dissolved in dry THF (1 mL), at 0 °C. After 30 min 10*H*-phenoxazine-10-carbonyl chloride (**25**, 246 mg, 1 mmol) dissolved in dry THF (1 mL) was added dropwise, and the resulting mixture was allowed to stir at room temperature overnight. The mixture was cooled to 0 °C and quenched with water (20 mL), and aqueous HCl solution (5 mL, 2 M) was added. The resulting solution was extracted with DCM (3 × 20 mL), and the combined organic layers were washed with saturated aqueous $NaHCO_3$ solution (50 mL) and brine (60 mL) and subsequently dried with $MgSO_4$ and evaporated to dryness.

General Procedure for the Synthesis of Compounds 34−45. A solution of the appropiate amine (1.62 mmol) was added to a solution of 10*H*-phenoxazine-10-carbonyl chloride (**25**, 200 mg, 0.81 mmol) in DCE (2 mL) at 0 °C under an argon atmosphere. The suspension was allowed to warm to room temperature and stirred for 2 h. Then the reaction was quenched with water (30 mL), and the aqueous portion was extracted with DCM (3 × 20 mL). The combined organic layers were washed with brine (50 mL), dried with $MgSO_4$, and evaporated. Pure compounds were isolated after crystallization (for crystallization solvents see the individual compounds).

General Procedure for the Synthesis of Compounds 49−52. Acridone (**8**, 394 mg, 2 mmol) was added portionwise to a stirred suspension of NaH (60% in mineral oil, 2.4 mmol, 96 mg) in dry dimethylformamide (DMF) (3.5 mL) at 0 °C under argon atmosphere. The resulting mixture was allowed to warm to room temperature and stirred for 1 h. Then a solution of benzyl chloride (3 mmol) in DMF (1.5 mL) was added and the mixture was stirred overnight. Water (30 mL) was added, and the resulting solution was extracted with ethyl acetate (3 × 20 mL). The combined organic extracts were washed with brine (60 mL) and dried with $MgSO_4$. Pure compounds were isolated after flash chromatography (for conditions see the individual compounds) and crystallized (for crystallization solvents see the individual compounds).

General Procedure for the Synthesis of Compounds 56 and 57. A suspension of 2-aminophenol (**54**, 218 mg, 2 mmol) and calcium carbonate (130 mg, 1.3 mmol) in dioxane (12 mL) was stirred at 70 °C for 80 min. Then carbonyl chloride (3.3 mmol) was added and the temperature was increased to 80 °C. After 90 min the mixture was filtered while hot and ice-cold water was added to the filtrate. The precipitate was filtered off, washed with 10 mL of ice cold water, and dried under high vacuum.

General Procedure for the Synthesis of Compounds 59−63. A solution of the carbamate (80.0 mg, 0.33 mmol), 1,2-dibromoethane (228 μL, 495.9 mg, 2.64 mmol), and potassium carbonate (912 mg, 6.60 mmol) in acetone (7 mL) was heated to reflux for 36 h. The reaction mixture was cooled to room temperature and filtered through Celite. Water (25 mL) and ethyl acetate (25 mL) were added, and the layers were separated. The aqueous layer was washed with ethyl acetate (2 × 25 mL), dried with $MgSO_4$, and evaporated. Pure compounds were isolated after flash chromatography (for conditions see the individual compounds).

(10*H*-Phenoxazin-10-yl)(phenyl)methanone (12). **12** was synthesized using benzoyl chloride (163 μL, 1.4 mmol). After flash chromatography (petroleum ether/ethyl acetate, 9:1) and crystallization (diethyl ether/DCM, 4:1) the product was obtained as a white powder (236 mg, 82% yield). ^{1}H NMR (500 MHz, $CDCl_3$) δ 7.44−7.43 (m, 2H), 7.38−7.35 (m, 3H), 7.27 (t, *J* = 8.0 Hz, 2H), 7.15−7.11 (m, 4H), 6.96−6.91 (m, 2H). ^{13}C NMR (126 MHz, $CDCl_3$) δ 168.2, 150.3, 135.0, 130.6, 130.1, 128.9, 128.1, 126.5, 124.7, 123.3, 116.6. LC−MS (*m*/*z*): positive mode 288 $[M + H]^+$, 575 $[2M + H]^+$. Purity by HPLC−UV (254 nm)−ESI-MS: 100.0%; mp 157−158 °C.

Isobutyl 10*H*-Phenoxazine-10-carboxylate (24). **24** was synthesized using isobutyl chloroformate (3 mL) at 110 °C for 3 h. After crystallization (hexane/ethyl acetate, 3:1) the product was obtained as a white powder (141 mg, 50% yield). ^{1}H NMR (500 MHz, $CDCl_3$) δ 7.55 (dd, *J* = 7.5, 1.5 Hz, 2H), 7.14 (td, *J* = 7.5, 1.5 Hz, 2H), 7.09 (td, *J* = 8.0, 1.5 Hz, 2H), 7.07 (dd, *J* = 8.0, 1.5 Hz, 2H), 4.04 (d, *J* = 6.5 Hz, 2H), 2.00 (m, 1H, CH), 0.95 (d, *J* = 6.5 Hz, 6H). ^{13}C NMR (126 MHz, $CDCl_3$) δ 153.5, 150.4, 128.7, 126.2, 125.0, 123.1, 116.6, 72.9, 27.8, 19.2. LC−MS (*m*/*z*): positive mode 284 $[M + H]^+$. Purity by HPLC−UV (254 nm)−ESI-MS: 100.0%; mp 82−83 °C.

Benzyl 10*H*-Phenoxazine-10-carboxylate (26). A solution of 10*H*-phenoxazine-10-carbonyl chloride (246 mg, 1 mmol) in benzyl alcohol (3 mL) was heated at 110 °C for 6 h. Then the reaction was quenched with water (30 mL), and then the aqueous portion was extracted with DCM (3 × 20 mL). The combined organic layers were washed with brine (60 mL). The organic phase was dried with $MgSO_4$ and evaporated. After flash chromatography (petroleum ether/ethyl acetate, 9:1) and crystallization (hexane/ethyl acetate, 3:1) the product was obtained as a white powder (151 mg, 48% yield). ^{1}H NMR (500 MHz, $CDCl_3$) δ 7.56 (dd, *J* = 8.0, 1.5 Hz, 2H), 7.40−7.32 (m, 5H), 7.14 (td, *J* = 7.5, 1.5 Hz, 2H), 7.10−7.05 (m, 4H), 5.30 (s, 2H). ^{13}C NMR (126 MHz, $CDCl_3$) δ 153.1, 150.4, 135.6, 128.6, 128.5, 128.3, 128.1, 126.4, 125.0, 123.2, 116.6, 68.3. LC−MS (*m*/*z*): positive mode 318 $[M + H]^+$. Purity by HPLC−UV (254 nm)−ESI-MS: 100.0%; mp 121−122 °C.

4-Methylbenzyl 10*H*-Phenoxazine-10-carboxylate (27). **27** was synthesized using 4-methylbenzyl alcohol (108 mg, 0.87 mmol). Crystallization from hexane/ethyl acetate, 3:1, afforded the product as a white powder (150 mg, 52% yield). ^{1}H NMR (500 MHz, $CDCl_3$) δ 7.55 (d, *J* = 7.5 Hz, 2H), 7.29 (d, *J* = 8.0 Hz, 2H), 7.18 (d, *J* = 7.5 Hz, 2H), 7.13 (td, *J* = 8.0, 1.5 Hz, 2H), 7.09−7.05 (m, 4H), 5.26 (s, 2H), 2.37 (s, 3H). ^{13}C NMR (126 MHz, $CDCl_3$) δ 153.2, 150.4, 138.2, 132.6, 129.2, 128.6, 128.3, 126.3, 125.0, 123.2, 116.6, 68.3, 21.2. LC−MS (*m*/*z*): positive mode 332 $[M + H]^+$. Purity by HPLC−UV (254 nm)−ESI-MS: 100.0%; mp 144−145 °C.

4-Chlorobenzyl 10*H*-Phenoxazine-10-carboxylate (28). **28** was synthesized using 4-chlorobenzyl alcohol (125 mg, 0.87 mmol). Crystallization from hexane/ethyl acetate, 3:1, afforded the product as a white powder (77 mg, 25% yield). ^{1}H NMR (500 MHz, $CDCl_3$) δ 7.52 (dd, *J* = 7.5, 1.3 Hz, 2H), 7.35−7.32 (m, 4H), 7.14 (td, *J* = 8.0, 1.5 Hz, 2H), 7.10−7.06 (m, 4H), 5.25 (s, 2H). ^{13}C NMR (126 MHz, $CDCl_3$) δ 153.0, 150.4, 134.3, 134.1, 129.6, 128.8, 128.4, 126.5, 124.9, 123.3, 116.7, 67.5. LC−MS (*m*/*z*): positive mode 352 $[M + H]^+$. Purity by HPLC−UV (254 nm)−ESI-MS: 100.0%; mp 182−183 °C.

4-Methoxybenzyl 10*H*-Phenoxazine-10-carboxylate (30). **30** was synthesized using 4-methoxybenzyl alcohol (110 mg, 0.87 mmol). Flash chromatography (petroleum ether/ethyl acetate, 93:7) and crystallization from hexane/ethyl acetate, 3:1, afforded the product as colorless needles (128 mg, 42% yield). ^{1}H NMR (500 MHz, $CDCl_3$) δ 7.53 (dd, *J* = 8.0, 1.5 Hz, 2H), 7.34 (d, *J* = 9.0 Hz, 2H), 7.13 (td, *J* = 7.5, 1.5 Hz, 2H), 7.08−7.04 (m, 4H), 6.90 (d, *J* = 8.5 Hz, 2H), 5.23 (s, 2H), 3.82 (s, 3H). ^{13}C NMR (126 MHz, $CDCl_3$) δ 159.7, 153.2, 150.4, 130.1, 128.6, 127.7, 126.3, 125.0, 123.2, 116.6, 113.9, 68.1, 55.3. LC−MS (*m*/*z*): negative mode 316 $[M - OCH_3]^-$. Purity by HPLC−UV (254 nm)−ESI-MS: 100.0%; mp 120−121 °C.

Phenethyl 10*H*-Phenoxazine-10-carboxylate (31). Phenylethyl alcohol (121 μL, 1 mmol) was added to a solution of 10*H*-phenoxazine-10-carbonyl chloride (246 mg, 1 mmol) dissolved in pyridine (2 mL), and the resulting solution was stirred at 90 °C for 4.5 h. Water (30 mL) was added, and the resulting solution was extracted with DCM (3 × 20 mL). The combined organic extracts were washed with brine (60 mL) and dried with $MgSO_4$. After crystallization from hexane/ethyl acetate, 3:1, the product was isolated as pale orange crystals (234 mg, 71% yield). ^{1}H NMR (500 MHz, $CDCl_3$) δ 7.41−7.39 (m, 2H), 7.31 (tt, *J* = 7.0, 1.5 Hz, 2H), 7.25 (tt, *J* = 7.5, 1.5 Hz,

dx.doi.org/10.1021/jm300845v | *J. Med. Chem.* 2012, 55, 9576−9588

1H), 7.22−7.20 (m, 2H), 7.15−7.11 (m, 2H), 7.06−7.02 (m, 4H), 4.48 (t, J = 6.5 Hz, 2H), 3.01 (t, J = 7.0 Hz, 2H). ^{13}C NMR (126 MHz, $CDCl_3$) δ 153.2, 150.4, 137.7, 129.0, 128.5, 128.5, 126.6, 126.3, 125.0, 123.2, 116.6, 67.3, 35.1. LC−MS (m/z): positive mode 332 $[M + H]^+$. Purity by HPLC−UV (254 nm)−ESI-MS: 100.0%; mp 78−80 °C.

***N*-Phenethyl-10*H*-phenoxazine-10-carboxamide (42).** **42** was synthesized using 2-phenylethylamine (254 μL, 2 mmol). After crystallization (hexane/ethyl acetate, 3:1) the product was obtained as a white powder (282 mg, 85% yield). ^{1}H NMR (500 MHz, $CDCl_3$) δ 7.36 (dd, J = 8.0, 1.5 Hz, 2H), 7.31−7.28 (m, 2H), 7.23 (td, J = 7.0, 1.5 Hz, 1H), 7.18−7.16 (m, 2H), 7.14−7.10 (m, 2H), 7.06−7.01 (m, 4H), 5.35 (t, J = 5.0 Hz, 1H, NH), 3.54 (q, J = 6.5 Hz, 2H), 2.85 (t, J = 7.0 Hz, 2H). ^{13}C NMR (126 MHz, $CDCl_3$) δ 154.5, 151.2, 138.9, 129.3, 128.8, 128.7, 126.5, 126.3, 124.5, 123.6, 117.0, 42.0, 35.7. LC−MS (m/z): positive mode 331 $[M + H]^+$, 661 $[2M + H]^+$. Purity by HPLC−UV (254 nm)−ESI-MS: 100.0%; mp 103−104 °C.

***N*,*N*-Dipropyl-10*H*-phenoxazine-10-carboxamide (43).** **43** was synthesized using *N*,*N*-dipropylamine (277 μL, 2 mmol). After crystallization (hexane/ethyl acetate, 3:1) the product was obtained as a pale yellow powder (197 mg, 64% yield). ^{1}H NMR (500 MHz, $CDCl_3$) δ 6.85−6.78 (m, 6H), 6.69−6.67 (m, 2H), 3.36 (t, J = 7.5 Hz, 4H), 1.65 (m, J = 7.5 Hz, 4H), 0.90 (t, J = 7.5 Hz, 6H). ^{13}C NMR (126 MHz, $CDCl_3$) δ 154.9, 144.4, 130.4, 123.7, 122.9, 116.1, 114.2, 50.0, 21.5, 11.5. LC−MS (m/z): positive mode 311 $[M + H]^+$, 621 $[2M + H]^+$. Purity by HPLC−UV (254 nm)−ESI-MS: 100.0%; mp 71−72 °C.

***N*-(2-Hydroxyphenyl)-2-(((1*R*,2*S*,5*R*)-2-isopropyl-5-methylcyclohexyl)oxy)acetamide (57).** **57** was synthesized using (−)-menthoxyacetyl chloride (2-(((1*R*,2*S*,5*R*)-2-isopropyl-5-methylcyclohexyl)oxy)acetyl chloride) (383 μL, 3.3 mmol). The product was isolated as a yellow solid (367 mg, 40% yield). ^{1}H NMR (500 MHz, $CDCl_3$) δ 9.11 (s, 1H), 8.60 (s, 1H), 7.13 (t, J = 8.4 Hz, 1H), 7.04−6.99 (m, 2H), 6.87 (t, J = 7.6 Hz, 1H), 4.25 (d, J = 15.6 Hz, 1H), 4.05 (d, J = 15.6 Hz, 1H), 3.28 (t, J = 10.6 Hz, 1H), 2.25−2.00 (m, 2H), 1.75−1.62 (m, 2H), 1.37 (dd, J = 12.3, 10.5 Hz, 2H), 0.96 (t, J = 7.0 Hz, 10H), 0.84 (d, J = 7.0 Hz, 3H). ^{13}C NMR (126 MHz, $CDCl_3$) δ 170.2, 148.7, 127.3, 124.8, 122.0, 120.3, 119.9, 81.1, 67.3, 48.0, 40.1, 34.3, 31.4, 26.3, 23.3, 22.2, 20.9, 16.3. LC−MS (m/z): positive mode 306 $[M + H]^+$. Purity by HPLC−UV (254 nm)−ESI-MS: 100.0%; mp 171−172 °C.

Biological Assays. 1321 N1 astrocytoma cell lines stably expressing the respective P2X receptor subtype were used for the assays. Chimeric P2X1 and P2X3 receptors were used in which the N-terminal domain and transmembrane domain I of the receptors were replaced by the analogous region of the P2X2 receptor, which abolished the fast desensitization kinetics typical for P2X1 and P2X3 receptors.[61,62]

Measurement of Intracellular Ca^{2+} in Transfected 1321N1 Astrocytoma Cells. P2X receptor function was determined by measuring ATP-mediated increases in cytosolic Ca^{2+} concentrations. The fluorescent Ca^{2+}-chelating dye Fluo-4 was used as an indicator of the relative levels of intracellular Ca^{2+} concentrations in a 96-well format using a fluorescence imaging plate reader (Novostar, BMG). Cells were grown to confluence in 96-well black-walled tissue culture plates and loaded with Fluo-4 AM (2.4 μM) in Hank's balanced salt solution (containing 10 mM HEPES, pH 7.3, and 1% Pluronic F127) for 1 h at 23 °C. After incubation the loaded cells were washed with the same buffer to remove extracellular Fluo-4 AM. Compound solutions were prepared in DMSO. Then an amount of 2 μL of compound dilutions was transferred into the measurement plate. Because of the low solubility of some of the compounds, the DMSO solution should be directly pipetted into the wells without prior dilution in buffer. The final DMSO concentration did not exceed 1%. Fluorescence intensity was measured at 520 nm for 30 s at 0.4 s intervals. Buffer or ATP solution was injected sequentially into separate wells using the automatic pipetting device. At least three independent experiments were performed, each in duplicate. Antagonists were added 30 min before the addition of the agonist ATP, applied at a concentration that corresponded to its EC_{80} value. The assay was performed in a final volume of 200 μL. Compounds were tested at seven to eight different concentrations.[63]

Radioligand Binding Studies. Membrane preparations of astrocytoma cells expressing hP2X4 receptors were obtained similarly as described before for Chinese hamster ovary cells expressing P2X4 receptors.[49] The competition binding studies were performed in assay buffer (50 mM Tris-HCl, pH 7.4) containing 1 mM EDTA and 0.2 nM [^{35}S]ATPγS. The incubations were started by the addition of membranes (10−15 μg) and were performed in a 250 μL final assay volume. The reactions were terminated by vacuum filtration over GF/B glass-fiber filters using a Brandell 48-well harvester. The filters were rinsed three times with ice-cold Tris-HCl buffer (50 mM, pH 7.4). The filters were punched out and transferred to 4 mL scintillation vials. Then 2.5 mL of Ultima Gold scintillation cocktail was added, and samples were counted after 6 h for 1 min each, using a liquid scintillation counter (LSC). Nonspecific binding of [^{35}S]ATPγS was determined using 100 μM ATP. All data were analyzed with GraphPad Prism, version 4.1 (GraphPad Inc., La Jolla, CA).

■ ASSOCIATED CONTENT

Ⓢ Supporting Information

Synthesis procedures and ^{1}H and ^{13}C NMR spectral data for compounds **10**, **11**, **13**−**23**, **25**, **29**, **32**−**40**, **43**−**53**, **55**, **56** and **58**−**63**; experimental procedures for investigating the hydrolytic stability of **26**; and results from additional biological assays. This material is available free of charge via the Internet at http://pubs.acs.org.

■ AUTHOR INFORMATION

Corresponding Author

*Phone: +49-228-73-2301. Fax: +49-228-73-2567. E-mail: christa.mueller@uni-bonn.de.

Notes

The authors declare no competing financial interest.

†On leave from the University of Al-Azhar, Assiut, Egypt.

■ ACKNOWLEDGMENTS

We thank Stefanie Weyler and Scarlett Weigel for expert technical assistance, Marion Schneider for LC−MS analyses, Sabine Terhart-Krabbe and Annette Reiner for NMR spectra, and Ralf Hausmann and Günter Schmalzing (University of Aachen, Germany) for the gift of some P2X receptor clones. This study was supported by the BMBF (German Federal Ministry for Education and Research) within the BioPharma initiative "Neuroallianz".

■ ABBREVIATIONSUSED

[^{35}S]ATPγS, [^{35}S]adenosine 5′-(γ-thio)triphosphate; 5-BDBD, 5-(3-bromophenyl)-1,3-dihydro-2*H*-benzofuro[3,2-*e*]-1,4-diazepin-2-one; BzATP, 2′,3′-*O*-(4-benzoylbenzoyl)adenosine 5′-triphosphate; HBSS, Hank's buffered salt solution; LLE, ligand-lipophilicity efficiency; 2-MeSATP, 2-methylthioadenosine 5-triphosphate; TNP-ATP, 2′,3′-*O*-(2,4,6-trinitrophenyl)-adenosine 5′-triphosphate

■ REFERENCES

(1) King, B. F. Molecular Biology of P2X Purinoceptors. In *Cardiovascular Biology of Purines*; Burnstock, G., Dobson, J. G., Laing, B. T., Linden, J., Eds.; Kluwer Academic Publications: Norwell, MA, 1998; pp 159−186.

(2) Ralevic, V.; Burnstock, G. Receptors for purines and pyrimidines. *Pharmacol. Rev.* **1998**, *50*, 413−492.

(3) Burnstock, G.; Williams, M. P2 Purinergic receptors: modulation of cell function and therapeutic potential. *J. Pharmacol. Exp. Ther.* **2000**, *295*, 862−869.

(4) Robson, S. C.; Sevigny, J.; Zimmermann, H. The E-NTPDase family of ectonucleotidases: structure function relationships and pathophysiological significance. *Purinergic Signalling* **2006**, *2*, 409−430.
(5) Fredholm, B. B.; IJzerman, A. P.; Jacobson, K. A.; Linden, J.; Müller, C. E. International Union of Basic and Clinical Pharmacology. LXXXI. Nomenclature and classification of adenosine receptors—an update. *Pharmacol. Rev.* **2011**, *63*, 1−34.
(6) Coddou, C. Activation and regulation of purinergic P2X receptor channels. *Pharmacol. Rev.* **2011**, *63*, 641−683.
(7) Burnstock, G. Physiology and pathophysiology of purinergic neurotransmission. *Physiol. Rev.* **2007**, *87*, 659−797.
(8) Fields, R. D.; Burnstock, G. Purinergic signalling in neuron-glia interactions. *Nat. Rev. Neurosci.* **2006**, *7*, 423−436.
(9) Burnstock, G.; De Ryck, M. UCB Pharma research day—25 October 2007 "Glia-neuron interactions and purinergic receptors in neurological disorders". *Purinergic Signalling* **2008**, *4*, 79−84.
(10) Burnstock, G. Purinergic signalling and disorders of the central nervous system. *Nat. Rev. Drug Discovery* **2008**, *7*, 575−590.
(11) Burnstock, G. Purinergic P2 receptors as targets for novel analgesics. *Pharmacol. Ther.* **2006**, *110*, 433−454.
(12) Kim, Y. C.; Brown, S. G.; Harden, T. K.; Boyer, J. L.; Dubyak, G.; King, B. F.; Burnstock, G.; Jacobson, K. A. Structure−activity relationships of pyridoxal phosphate derivatives as potent and selective antagonists of P2X1 receptors. *J. Med. Chem.* **2001**, *44*, 340−349.
(13) Baqi, Y.; Hausmann, R.; Rosefort, C.; Rettinger, J.; Schmalzing, G.; Müller, C. E. Discovery of potent competitive antagonists and positive modulators of the P2X2 Receptor. *J. Med. Chem.* **2011**, *54*, 817−830.
(14) Wolf, C.; Rosefort, C.; Fallah, G.; Kassack, M. U.; Hamacher, A.; Bodnar, M.; Wang, H.; Illes, P.; Kless, A.; Bahrenberg, G.; Schmalzing, G.; Hausmann, R. Molecular determinants of potent P2X2 antagonism identified by functional analysis, mutagenesis, and homology docking. *Mol. Pharmacol.* **2011**, *79*, 649−661.
(15) Volpini, R.; Mishra, R. C.; Kachare, D. D.; Dal Ben, D.; Lambertucci, C.; Antonini, I.; Vittori, S.; Marucci, G.; Sokolova, E.; Nistri, A.; Cristalli, G. Adenine-based acyclic nucleotides as novel P2X3 receptor ligands. *J. Med. Chem.* **2009**, *52*, 4596−4603.
(16) Jahangir, A.; Alam, M.; Carter, D. S.; Dillon, M. P.; Du Bois, D. J.; Ford, A. P. D. W.; Gever, J. R.; Lin, C.; Wagner, P. J.; Zhai, Y.; Zira, J. Identification and SAR of novel diaminopyrimidines. Part 2: The discovery of RO-51, a potent and selective, dual P2X3/P2X2/3 antagonist for the treatment of pain. *Bioorg. Med. Chem. Lett.* **2009**, *19*, 1632−1635.
(17) Lee, W. G.; Lee, S. D.; Cho, J. H.; Jung, Y.; Kim, Y. H.; Hien, T. T.; Kang, K. W.; Ko, H.; Kim, Y. C. Structure−activity relationships and optimization of 3,5-dichloropyridine derivatives as novel P2X7 receptor antagonists. *J. Med. Chem.* **2012**, *55*, 3687−3698.
(18) Baraldi, P. G.; Nuñez, M. C.; Morelli, A.; Falzoni, S.; Di Virgilio, F.; Romagnoli, R. Synthesis and biological activity of *N*-arylpiperazine-modified analogues of KN-62, a potent antagonist of the purinergic P2X7 receptor. *J. Med. Chem.* **2003**, *46*, 1318−1329.
(19) Kawate, T.; Michel, J. C.; Birdsong, W. B.; Gouaux, E. Crystal structure of the ATP-gated P2X4 ion channel in the closed state. *Nature* **2009**, 592−598.
(20) Samwaysa, D. S. K.; Khakhb, B. S.; Dutertrec, S.; Egan, E. M. Preferential use of unobstructed lateral portals as the access route to the pore of human ATP-gated ion channels (P2X receptors). *Proc. Natl. Acad. Sci. U.S.A.* **2011**, *108*, 13800−13805.
(21) Du, J.; Dong, H.; Zhou, H. X. Gating mechanism of a P2X4 receptor developed from normal mode analysis and molecular dynamics simulations. *Proc. Natl. Acad. Sci. U.S.A.* **2012**, *109*, 4140−4145.
(22) Tsuda, M.; Shigemoto-Mogami, Y.; Koizumi, S.; Mizokoshi, A.; Kohsaka, S.; Salter, M. W.; Inoue, K. P2X4 receptors induced in spinal microglia gate tactile allodynia after nerve injury. *Nature* **2003**, *424*, 778−783.
(23) Guo, L.; Trautmann, K.; Schluesener, H. J. Expression of P2X4 receptor by lesional activated microglia during formalin-induced inflammatory pain. *J. Neuroimmunol.* **2005**, *163*, 120−127.
(24) Ulmann, L.; Hatcher, J. P.; Hughes, J. P.; Chaumont, S.; Green, P. J.; Conquet, F.; Buell, G. N.; Reeve, A. J.; Chessell, I. P.; Rassendren, F. Up-regulation of P2X4 receptors in spinal microglia after peripheral nerve injury mediates BDNF release and neuropathic pain. *J. Neurosci.* **2008**, *28*, 11263−11268.
(25) Zhang, Z.; Artelt, M.; Burnet, M.; Trautmann, K.; Schluesener, H. J. Lesional accumulation of P2X4 receptor monocytes following experimental traumatic brain injury. *Exp. Neurol.* **2006**, *197*, 252−257.
(26) Cavalieri, F.; Florenzano, F.; Amadio, S.; Fusco, F. R.; Viscomi, M. T.; D'Ambrosi, N.; Vacca, F.; Sancesario, G.; Bernardi, G.; Molinari, M.; Volontè, C. Up-regulation of P2X2, P2X4 receptor and ischemic cell death: prevention by P2 antagonists. *Neuroscience* **2003**, *120*, 85−98.
(27) Schwab, J. M.; Guo, L.; Schluesener, H. J. Spinal cord injury induces early and persistent lesional P2X(4) receptor expression. *J. Neuroimmunol.* **2005**, *163*, 185−189.
(28) Sandkühler, J. Models and mechanisms of hyperalgesia and allodynia. *Physiol. Rev.* **2009**, *89*, 707−758.
(29) Tsuda, M.; Kuboyama, K.; Inoue, T.; Nagata, K.; Tokazi-Saitoh, H.; Inoue, K. Behavioral phenotypes of mice lacking purinergic P2X4 receptors in acute and chronic pain assays. *Mol. Pain* **2009**, *5*, 28.
(30) Buell, G.; Lewis, C.; Collo, G.; North, R. A.; Surprenant, A. An antagonist-insensitive P2X receptor expressed in epithelia and brain. *EMBO J.* **1996**, *15*, 55−62.
(31) Soto, F.; Garcia-Guzman, M.; Gomez-Hernandez, J. M.; Hollmann, M.; Karschin, C.; Stühmer, W. P2X4: an ATP-activated ionotropic receptor cloned from rat brain. *Proc. Natl. Acad. Sci. U.S.A.* **1996**, *93*, 3684−3688.
(32) Jones, C. A.; Chessell, I. P.; Simon, J.; Barnard, E. A.; Miller, K. J.; Michel, A. D.; Humphrey, P. P. *Br. J. Pharmacol.* **2000**, *129*, 388−394.
(33) He, M. L.; Gonzalez-Iglesias, A. E.; Stojilkovic, S. S. Functional characterization of the P2X4 receptor orthologues. *J. Biol. Chem.* **2003**, *278*, 46270−46277.
(34) Bo, X.; Liu, M.; Schoepfer, R.; Burnstock., G. Characterization and expression of ATP P2X4 receptor from embryonic chick skeletal muscle. *Drug Dev. Res.* **2001**, *53*, 22−28.
(35) Virginio, C.; Robertson, G.; Surprenant, A.; North, R. A. Trinitrophenyl-substituted nucleotides are potent antagonists selective for P2X1, P2X3, and heteromeric P2X2/3 receptors. *Mol. Pharmacol.* **1998**, *53*, 969−973.
(36) Nagata, K.; Imai, T.; Yamashita, T.; Tsuda, M.; Tozaki-Saitoh, H.; Inoue, K. Antidepressants inhibit P2X4 receptor function: a possible involvement in neuropathic pain relief. *Mol. Pain* **2009**, *5*, 20.
(37) Toulme, E.; Garcia, A.; Samways, D.; Egan, T. M.; Carson, M. J.; Khakh, B. S. P2X4 receptors in activated C8-B4 cells of cerebellar microglial origin. *J. Gen. Physiol.* **2010**, *135*, 333−353.
(38) Donnelly-Roberts, D.; McGaraughty, S.; Shieh, C. C.; Honore, P.; Jarvis, M. F. Painful purinergic receptors. *J. Pharmacol. Exp. Ther.* **2008**, *324*, 409−415.
(39) Hajieva, P.; Mocko, J. B.; Moosmann, B.; Behl, C. Novel imine antioxidants at low nanomolar concentrations protect dopaminergic cells from oxidative neurotoxicity. *J. Neurochem.* **2009**, *110*, 118−132.
(40) Behl, C.; Moosmann, B. Oxidative nerve cell death in Alzheimer's disease and stroke: antioxidants as neuroprotective compounds. *Biol. Chem.* **2002**, *383*, 521−536.
(41) Thimmaiah, K. N.; Horton, J. K.; Seshadri, R.; Israel, M.; Houghton, J. A.; Harwood, F. C.; Houghton, P. J. Synthesis and chemical characterization of N-substituted phenoxazines directed toward reversing vinca alkaloid resistance in multidrug-resistant cancer cells. *J. Med. Chem.* **1992**, *35*, 3358−3364 and references cited herein..
(42) Thimmaiah, K. N.; Easton, J. B.; Germain, G. S.; Morton, C. L.; Kamath, S.; Buolamwini, J. K.; Houghton, P. J. Identification of N^{10}-substituted phenoxazines as potent and specific inhibitors of Akt signaling. *J. Biol. Chem.* **2005**, *280*, 31924−31935.
(43) Kivlehan, F.; Lefoix, M.; Moynihan, H. A.; Thompson, D.; Ogurtsov, V. I.; Herzog, G.; Arrigan, D. W. M. Interaction of acridine-calix[4]arene with DNA at the electrified liquidlliquid interface. *Electrochim. Acta* **2010**, *55*, 3348−3354.

(44) Nishimura, T.; Katoh, T.; Hayashi, T. Rhodium-catalyzed aryl transfer from trisubstituted aryl methanols to alpha,beta-unsaturated carbonyl compounds. *Angew. Chem., Int. Ed.* **2007**, *46*, 4937−4939.
(45) Gao, C.; Jiang, Y.; Tan, C.; Zu, X.; Liu, H.; Cao, D. Synthesis and potent antileukemic activities of 10-benzyl-9(10*H*)-acridinones. *Bioorg. Med. Chem.* **2008**, *16*, 8670−8675.
(46) Wang, C.; Hang, T.; Zhang, H. Microwave-promoted N-alkylation of acridones without solvent. *Synth. Commun.* **2003**, *33*, 451−456.
(47) Lee, G. E.; Joshi, B. V.; Chen, W.; Jeong, L. S.; Moon, H. R.; Jacobson, K. A.; Kim, Y. C. Synthesis and structure−activity relationship studies of tyrosine-based antagonists at the human P2X7 receptor. *Bioorg. Med. Chem. Lett.* **2008**, *18*, 571−575.
(48) Michel, A. D.; Ng, S. W.; Roman, S.; Clay, W. C.; Dean, D. K.; Walter, D. S. Mechanism of action of species-selective P2X7 receptor antagonists. *Br. J. Pharmacol.* **2009**, *156*, 1312−1325.
(49) Michel, A. D.; Miller, K. J.; Lundström, K.; Buell, G. N.; Humphrey, P. P. Radiolabeling of the rat P2X4 purinoceptor: evidence for allosteric interactions of purinoceptor antagonists and monovalent cations with P2X purinoceptors. *Mol. Pharmacol.* **1997**, *51*, 524−532.
(50) Bordell, F.; Hughes, D. L. S_N2 reactions of nitranions with benzyl chlorides. *J. Am. Chem. Soc.* **1984**, *106*, 3234−3240.
(51) Müller, P; Buu-Hoi, N. P.; Rips, R. Preparation and reactions of phenoxazine and phenoselenazine. *J. Org. Chem.* **1959**, *24*, 37−39.
(52) Fischer, H.; Buergin, W. Microbicidal Dibenzazoles. CH 653675 A5 19860115, 1986, .
(53) Burmistrov, S. I.; Karpishenko, L. S. Synthesis of benzene-sulfonyl derivatives of phenoxazine. *Khim. Geterotsikl.* **1974**, *11*, 1576−1577.
(54) Samolovova, V. G.; Gortinskaya, T. V.; Shchukina, M. N. Phenoxazine series. VI. Synthesis of some 10-substituted phenoxazines. *Zh. Obshch. Khim.* **1962**, *32*, 1085−1088.
(55) Gal, A. E.; Avakian, S. Nitrogen substituted phenoxazines. *J. Med. Chem.* **1963**, *6*, 809−811.
(56) Chen, G.-S. J.; Gibson, M. S. Synthesis of 10-benzoyl-9-acridone and 9-acridone from 2,2′- and 2,3′-disubstituted benzophenones. *J. Chem. Soc., Perkin Trans. 1* **1975**, *12*, 1138−1139.
(57) Wagner, G.; Leistner, S. Effects of amines and hydrazines on benzoxazolinone and benzoxalinethione. *Pharmazie* **1976**, *31*, 345−347.
(58) Faler, C. A.; Joullie, M. M. Aminolysis of allyl esters with bislithium aryl amides. *Tetrahedron Lett.* **2006**, *47*, 7229−7231.
(59) Chabrier, P.; Najer, H.; Giudicelli, R. New carbamates with local anesthetic activity. II. Derivatives of *p*-aminophenol and *o*-aminophenol. *Bull. Soc. Chim. Fr.* **1955**, 1353−1362.
(60) Coudert, G.; Guillaumet, G.; Loubinoux, B. A new synthesis of 3,4-dihydro-2*H*-1,4-benzoxazines using solid-liquid phase-transfer catalysis. *Synthesis* **1979**, *7*, 541−543.
(61) Neelands, T. R.; Burgard, E. C.; Uchic, M. E.; McDonald, H. A.; Niforatos, W.; Faltynek, C. R.; Lynch, K. J.; Jarvis, M. F. 2′,3′-*O*-(2,4,6,Trinitrophenyl)-ATP and A-317491 are competitive antagonists at a slowly desensitizing chimeric human P2X3 receptor. *Br. J. Pharmacol.* **2003**, *140*, 202−210.
(62) Rettinger, J.; Schmalzing, G. Desensitization masks nanomolar potency of ATP for the P2X1 receptor. *J. Biol. Chem.* **2004**, *279*, 6426−6433.
(63) Gee, K. R.; Brown, K. A.; Chen, W. N.; Bishop-Stewart, J.; Gray, D.; Johnson, I. Chemical and physiological characterization of Fluo-4 Ca^{2+} indicator dyes. *Cell Calcium* **2000**, *27*, 97−106.